

Direct numerical simulation of natural convection in a vertical channel

C. S. Ng, D. Chung and A. Ooi

Department of Mechanical Engineering
 The University of Melbourne, Victoria 3010, AUSTRALIA

Abstract

This study presents direct numerical simulations of natural convection for air ($Pr = 0.709$) in a vertical channel driven by differentially heated walls at Rayleigh numbers (Ra) up to 2.0×10^7 . The present data is validated with that from Versteegh and Nieuwstadt [9] for $Ra = 5.0 \times 10^6$. Using the present data for higher Ra , we appraise and compare the various proposed scaling laws for the mean temperature defect, $T_h - \bar{T}$, and the streamwise velocity, \bar{u} , by Versteegh and Nieuwstadt [9], Hölling and Herwig [2] and Shiri and George [6] (cf. George and Capp [1]). For the mean temperature profile, the present data supports the inner temperature scaling, $T_i = [|f_w|^3 / (g\beta\alpha)]^{1/4}$, proposed by all the three studies, where f_w is the heat flux at the wall, g is the gravitational acceleration, β is the thermal expansion coefficient and α is the heat diffusion coefficient. Using compensated temperature gradients, constants are found for the wall function for mean temperature, which takes the form of a power-law:

$$\frac{T_h - \bar{T}}{T_i} = -3.6 \left(\frac{z}{l_i} \right)^{-1/3} + 4.5,$$

where z is the distance in the wall-normal direction and l_i is the inner length scale, defined by $[\alpha^3 / (g\beta|f_w|)]^{1/4}$. For the mean velocity profile, we found that the inner velocity scale $u_i = (g\beta|f_w|h)^{1/3}$, proposed by Shiri and George [6], collapses the velocity profiles in the near-wall region. Here, we define h as the channel half-width.

Introduction

Statistics describing turbulent natural convection in a vertical channel have, in the past, been approached through various forms of scaling analysis (e.g. George and Capp [1], Shiri and George [6], Hölling and Herwig [2], Yuan *et al.* [10]), and is typically followed by validation with experimental and DNS data (e.g. Versteegh and Nieuwstadt [9]). Hereafter, with the exception of Yuan *et al.*, we refer to the authors as GC, SG, HH and VN respectively.

To date, the DNS data by VN for Ra up to 5.0×10^6 and the experimental data by Tsuji and Nagano [8] for Ra up to 2.5×10^{11} are the known highest- Ra data available for comparison. However, as DNS enables a more straightforward collation of data for higher-order statistics, this paper focuses on providing DNS data for $Ra > 5.0 \times 10^6$ to validate proposed scaling laws and asymptotic theories. Furthermore, SG argues that, in order for deductions of asymptotic wall functions to be critically evaluated, channel flow should ideally have a ratio of outer to inner length scales, h/l_i , greater than 10. We use this ratio as a starting point for comparison. For the present data, h/l_i is in the range of 19–62.

Background

Governing Equations

For the present study, we adopt the Boussinesq approximation (constant fluid properties except buoyancy, which is a function

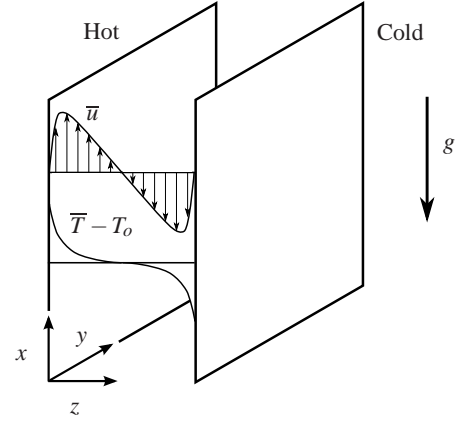


Figure 1: Diagram of natural convection in a vertical channel.

of temperature) for fully developed turbulent natural convection flow driven by the temperature difference between the two walls, ΔT . Here, $\Delta T = T_h - T_c$, where T_h and T_c are defined as the temperatures of the ‘hot’ and ‘cold’ walls respectively. For all simulations in this study, the ‘hot’ wall is defined as the left channel wall (figure 1). T_0 is defined as the average temperature across the channel. The relevant measure of the flow, analogous to the Reynolds number, is the Rayleigh number Ra , defined as $Ra = g\beta\Delta T h^3 / (\nu\alpha)$, where g is the acceleration of gravity, ν is the viscosity, α is the thermal diffusivity and β is the thermal expansion coefficient. ν , α and β are properties of the fluid in the channel. The streamwise, spanwise and wall-normal directions are x , y and z respectively, and the channel full width is h ($= 2h$). The mean equations of motion can be written as:

$$0 = \frac{d}{dz} \left(\nu \frac{d\bar{u}}{dz} - \overline{u'w'} \right) + g\beta(\bar{T} - T_0), \quad (1)$$

$$0 = \frac{d}{dz} \left(\alpha \frac{d\bar{T}}{dz} - \overline{w'T'} \right), \quad (2)$$

(cf. GC) where the mean flow is averaged over time as well as the streamwise and spanwise direction. The overbar denotes the ensemble average of the quantities while the fluctuating quantities are denoted by a prime. The Reynolds stress is $-\overline{u'w'}$ and the turbulent heat flux is $-\overline{w'T'}$.

Simulation Details

The governing equations are solved numerically over a computational domain size defined by $L_x \times L_y \times L_z$, with resolutions $n_x \times n_y \times n_z = 432 \times 216 \times 96$ for Ra up to 5.0×10^6 (cf. VN) and $n_x \times n_y \times n_z = 768 \times 384 \times 192$ for $Ra = 2.0 \times 10^7$. We have determined that grid spacings, $\Delta x/l_i$ of $O(1)$ are sufficient to resolve the small scales. The simulation time is defined as $t_{sim}/t_{eddy} = ((g\beta f_w h)^{1/3} \cdot t_{sim})/h$, (see table 2:SG), where t_{sim} is the length of time used to record statistics. Table 1 lists the simulation parameters in this study.

The governing equations are spatially discretised using the fully

Ra	L_x/h	L_y/h	Δx^\times	Δy^\times	Δz_c^\times	$t_{\text{sim}}/t_{\text{eddy}}$
5.4×10^5	24	12	1.1	1.1	0.6	120.0
2.0×10^6	24	12	1.6	1.6	1.0	147.1
5.0×10^6	24	12	2.2	2.2	1.3	117.3
$\dagger 2.0 \times 10^7$	24	12	1.9	1.9	1.0	12.8

Table 1: Simulation parameters for this study. The cell grid-sizes, Δx^\times , Δy^\times and Δz_c^\times are scaled by the inner length scale, $l_i = [\alpha^3/(g\beta|f_w|)]^{1/4}$. The wall normal gridsize Δz_c^\times is measured at the channel half-width. (\dagger At the time of writing, the highest Ra appears not to have fully converged ($t_{\text{sim}}/t_{\text{eddy}} < 100.0$), but the results are included nonetheless.)

conservative fourth-order staggered scheme of Morinishi *et al.* [4] and marched in time using the low-storage third-order Runge–Kutta scheme of Spalart *et al.* [7]. The velocity field is projected onto a divergence-free field after each Runge–Kutta stage via the fractional-step method (e.g. Kim and Moin [3]). Grid spacings in the streamwise and spanwise directions are uniform, and the wall-normal spacings utilise a cosine stretching grid.

Comparison with Published DNS Data

The results of the present DNS are validated against the data of VN. Flow statistics for $Ra = 5.0 \times 10^6$ are shown in figures 2 and 3.

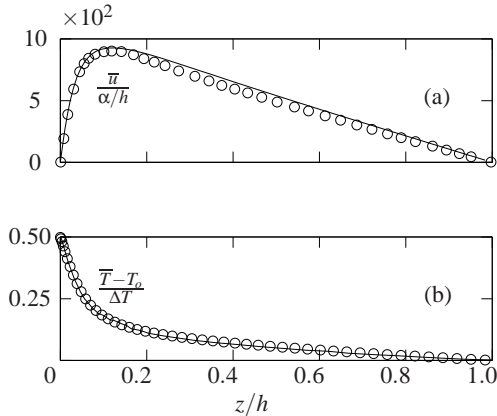


Figure 2: DNS temperature and velocity data for $Ra = 5.0 \times 10^6$ by VN [9] (\circ) compared with the present data ($—$).

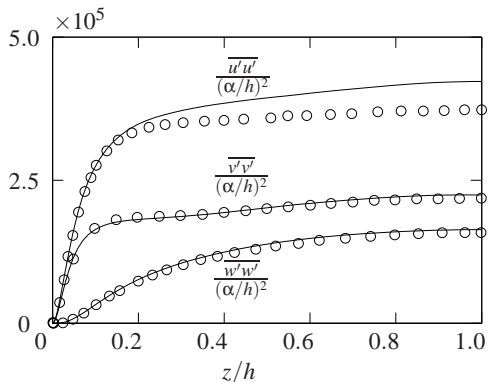


Figure 3: DNS turbulent velocity data for $Ra = 5.0 \times 10^6$ by VN [9] (\circ) compared with the present data ($—$).

In the mean temperature plot (figure 2b), the present data

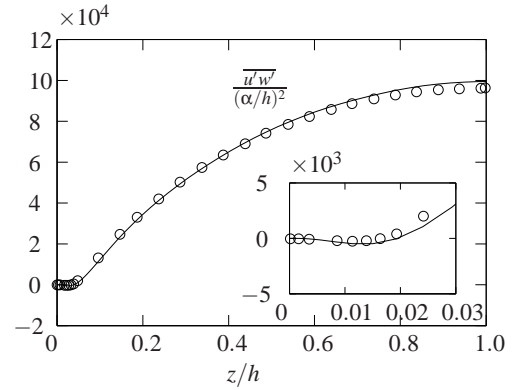


Figure 4: DNS cross-correlated turbulent velocity data for $Ra = 5.0 \times 10^6$ by VN [9] (\circ) compared with the present data ($—$). The inset figure shows DNS data for z/h up to 0.03.

matches well with the data from VN. However, for the mean velocity (figure 2a), the streamwise velocity data from the present simulation exhibits a higher peak velocity, at ($z/h \approx 0.1$, $\bar{u}/(\alpha/h) \approx 930$) compared to data by VN at (≈ 0.1 , ≈ 900). Similarly for the turbulent streamwise velocity (figure 3, top curve), the present simulation data peak at the centre of the channel at ($z/h \approx 1.0$, $\overline{u'u'}/(\alpha/h)^2 \approx 4.2 \times 10^5$) compared to data by VN at (≈ 1.0 , $\approx 3.7 \times 10^5$). The spanwise, wall-normal and cross-correlated turbulent velocity fluctuations ($\overline{u'w'}/(\alpha/h)^2$) matches to that of VN (the latter shown in figure 4). At the time of writing, the cause of the difference for the streamwise velocity data is still unknown but, in general, the present simulations agree qualitatively with the DNS data of VN.

Analysis of High Rayleigh Number Results

Temperature Profile

We begin by describing the inner–outer scaling approach adopted by the various authors named above, which defines an inner layer of the flow close to the wall and an outer layer at the core of the channel. Equation (2) can be integrated, giving

$$\alpha \frac{d\bar{T}}{dz} - \overline{w'T'} = -\frac{q_w}{\rho C_p} \equiv -f_w, \quad (3)$$

which describes a characteristic heat flux constant f_w equivalent to the wall heat flux q_w flowing from left to right divided by density ρ and specific heat C_p . The same constant heat flux is felt by both inner and outer regions of the flow. This implies that the characteristic constant f_w is independent of location and can be deduced as a characteristic parameter for describing the flow in the channel. From equations (1) and (2), the parameters α , ν , $g\beta$ and h , are used to form the necessary scales (cf. GC). The inner scaling for temperature and length proposed by VN, HH and SG (cf. GC) are summarised in table 2.

All three studies propose similar inner and outer length scales, as well as the inner temperature scale. However, there are differences in the choice of the velocity scales and the outer temperature scales. These differences potentially arose from the limited availability of high Ra data to date.

Interestingly, but not surprisingly, the wall functions proposed are different: VN and SG (cf. GC) propose a power-law function based on dimensional arguments positing the existence of a buoyant sublayer while HH proposes a logarithmic law using the gradient-matching approach. Of the three, SG did not determine a constant for their wall function.

	VN [9]	HH [2]	SG [6]
<i>Inner scaling</i>			
u_i	$(g\beta f_w \alpha)^{1/4}$	$(g\beta f_w \alpha)^{1/4}Pr^{-1}$	$(g\beta f_w h)^{1/3}$
T_i	$\left(\frac{ f_w ^3}{g\beta\alpha}\right)^{1/4}$	$\left(\frac{ f_w ^3}{g\beta\alpha}\right)^{1/4}$	$\left(\frac{ f_w ^3}{g\beta\alpha}\right)^{1/4}$
l_i	$\left(\frac{\alpha^3}{g\beta f_w }\right)^{1/4}$	$\left(\frac{\alpha^3}{g\beta f_w }\right)^{1/4}$	$\left(\frac{\alpha^3}{g\beta f_w }\right)^{1/4}$
<i>Outer scaling</i>			
u_o	$(g\beta f_w h)^{1/3}$	$(g\beta f_w \alpha)^{1/4}Pr^{-1}$	$(g\beta f_w h)^{1/3}$
T_o	$\left(\frac{ f_w ^2}{g\beta h}\right)^{1/3}$	$\left(\frac{ f_w ^3}{g\beta\alpha}\right)^{1/4}$	$\left(\frac{ f_w ^2}{g\beta h}\right)^{1/3}$
l_o	h	h	h

Table 2: Comparison of inner and outer layer scales.

Using the present data, we now determine the constants for the temperature wall function proposed by SG, which takes the power-law form:

$$\frac{T_h - \bar{T}}{T_i} = -c_1 \left(\frac{z}{l_i}\right)^{-1/3} - c_2(Pr), \quad (4)$$

where c_1 is a constant yet to be determined and $c_2(Pr)$ is a Prandtl number dependent constant. Presently, $c_2(Pr)$ is constant for $Pr = 0.709$. By differentiating equation (4), we obtain

$$\frac{dT^\times}{dz^\times} = \left(\frac{c_1}{3}\right)(z^\times)^{-4/3}, \quad (5)$$

where $T^\times = (T_h - \bar{T})/T_i = (T_h - \bar{T})/[|f_w|^3/(g\beta\alpha)]^{1/4}$ and $z^\times = z/l_i = z/[\alpha^3/(g\beta|f_w|)]^{1/4}$. To estimate the constants c_1 and c_2 , we rewrite equations (4) and (5) into diagnostic quantities, $c_1 = 3z^{\times(4/3)}dT^\times/dz^\times$ and $c_2 = -3z^\times dT^\times/dz^\times - T^\times$, similar to the approach by Moser *et al.*[5]. Assuming that the power law is valid, c_1 and c_2 should exhibit linearity in a region of z^\times , which we estimated in figure 5 for $1 \lesssim z^\times \lesssim 3$.

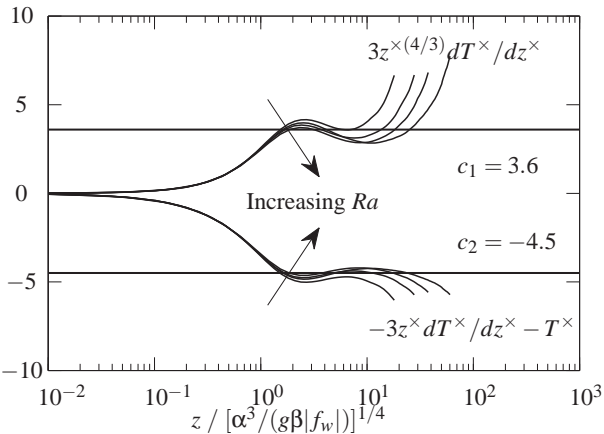


Figure 5: A plot of compensated temperature gradient to determine the universal constants c_1 and c_2 .

Hence, we determine the constants to be: $c_1 = 3.6$ and $c_2 = -4.5$, giving the temperature wall function with newly fitted constants:

$$\frac{T_h - \bar{T}}{T_i} = -3.6 \left(\frac{z}{l_i}\right)^{-1/3} + 4.5. \quad (6)$$

In summary, the wall functions are listed in table 3.

VN [9] (cf. GC [1])	$-4.2(z^\times)^{-1/3} + 5.0$
HH [2]	$0.4 \log(z^\times) + 1.9$
SG [6]	$-3.6(z^\times)^{-1/3} + 4.5^*$

Table 3: Temperature wall functions, $T^\times(z^\times)$. For (*), constants are determined from present data.

Figure 6 compares the fit of the respective wall functions to the present DNS data. As expected, the linear region near the wall, $T^\times = z^\times$ fits the profiles exactly, up to $z^\times \approx 1$. However, we found that each outer wall functions fit different ranges of the temperature profile. The logarithmic equation of HH appears to fit the outer region $7 \lesssim z^\times \lesssim 30$ while the power-law equation of VN fits the lowest Ra data very well. In contrast, the power-law function with new constants (a variation from VN and GC) shows a good fit to the DNS data from $z^\times \approx 1$ to $z^\times \approx 30$ with a slight deviation between $2.5 \lesssim z^\times \lesssim 10$ and it appears that the trend will continue asymptotically.

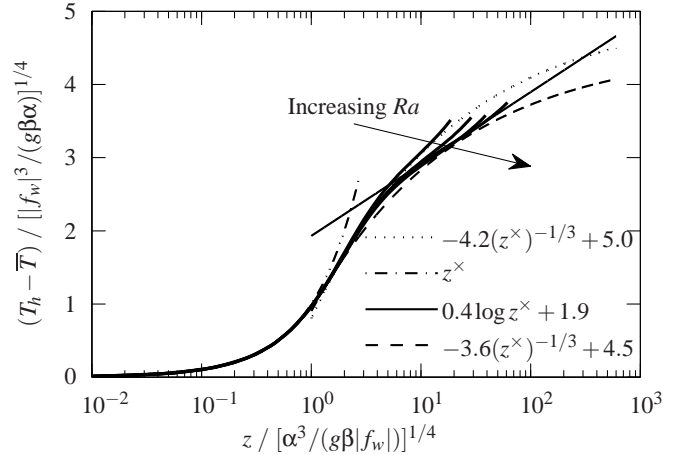


Figure 6: DNS temperature data scaled with inner temperature scale, T_i , and inner length scale, l_i , showing general agreement with new temperature wall function for $1 \lesssim z^\times \lesssim 30$, with slight deviation between $2.5 \lesssim z^\times \lesssim 10$.

Velocity Profile

Here, we shall perform a straightforward comparison and appraisal of inner velocity scales using the present data. In addition, and of particular interest, is the asymptotic velocity profile theory proposed by SG which we also used to analyse the present data. For reference, the velocity scales are summarised in table 2.

VN and HH approached the problem of inner velocity scaling on the assumption that local effects drive the flow close to the wall, so on dimensional grounds, $u_{iT} = (g\beta|f_w|\alpha)^{1/4}$. Here, the subscript T identifies a velocity scale based on thermal diffusivity, α . Plotting the data from this study with u_{iT} gives figure 7. In the region close to the wall ($z^\times < 1$) where the velocity profiles are expected to collapse, we observe a systematic departure with increasing Ra .

SG, however, argues that asymptotically, the buoyancy-induced flow away from the wall drives the velocity in the vicinity of the wall. In other words, the outer velocity scaling $u_{oh} = (g\beta|f_w|h)^{1/3}$ matches the inner velocity scaling u_{ih} for sufficiently high Ra values. The subscript h denotes dependency on the outer flow region. This is apparent in figure 8, where a

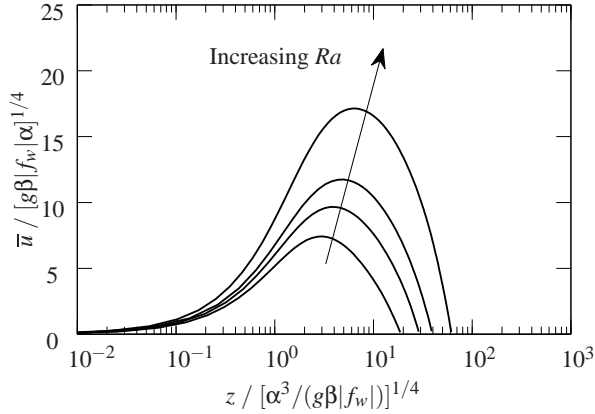


Figure 7: DNS velocity data scaled with inner velocity scale, u_{iT} , and inner length scale, l_i , showing systematic increase with higher Ra .

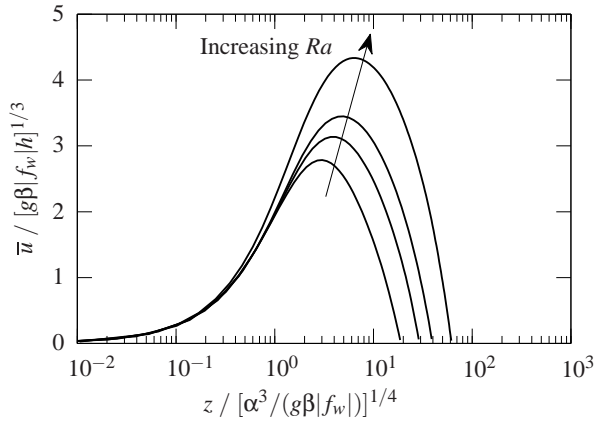


Figure 8: DNS velocity data scaled with inner velocity scale, u_{ih} and inner length scale, l_i , showing collapse of velocity profiles for z^\times up to 0.3.

collapse of the velocity profiles is apparent for $z^\times < 0.3$.

In the asymptotic analysis of the inner velocity scale, SG and GC theorised a proportional relationship between the velocity scale, u_{oh} , and the wall shear velocity, u_τ , as $Ra \rightarrow \infty$, that is, the ratio u_τ/u_{oh} approaches a constant for sufficiently high Ra . With the present data, we calculate u_τ/u_{oh} and a plot against $\log(Ra)$ is shown in figure 9. From the figure, we observe a decreasing trend that appears to approach a constant. This suggests that perhaps, the present Ra is not sufficiently high to test the theory proposed by SG and GC. This is subject to ongoing investigation.

Conclusions

DNS for turbulent natural convection in a vertical channel for Ra up to 2.0×10^7 was conducted, and data for $Ra = 5.0 \times 10^6$ was validated with published results from Versteegh and Nieuwstadt [9]. Using the present data, new constants for the asymptotic temperature wall function have been determined and appears to support a power law. For the mean velocity profile, the data for high Ra collapses with the velocity scale proposed by Shiri and George [6], which supports the theory that the near wall flow regime is dependent on buoyant effects away from the wall. From this finding, Shiri and George [6]'s proposed relationship between the wall shear velocity, u_τ , and the velocity scale, u_{oh} at higher Ra has interesting implications: a log-

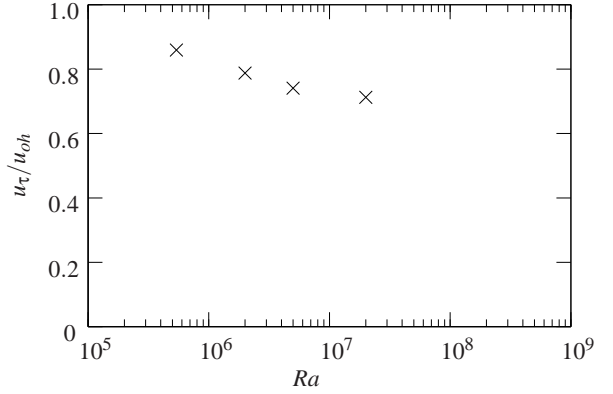


Figure 9: A plot of u_τ/u_{oh} versus $\log Ra$ showing potential convergence with increasing Ra .

arithmic relationship for the mean velocity profile. This is the subject of our ongoing study.

References

- [1] George, W. K. J. and Capp, S. P., A theory for natural convection turbulent boundary layers next to heated vertical surfaces, *Int. J. Heat Mass Transfer*, **22**, 1979, 813–826.
- [2] Hölling, M. and Herwig, H., Asymptotic analysis of the near-wall region of turbulent natural convection flows, *J. Fluid Mech.*, **541**, 2005, 383–397.
- [3] Kim, J. and Moin, P., Application of a fractional-step method to incompressible Navier–Stokes equations, *J. Comput. Phys.*, **59**, 1985, 308–323.
- [4] Morinishi, Y., Lund, T. S., Vasilyev, O. V. and Moin, P., Fully conservative higher order finite difference schemes for incompressible flow, *J. Comput. Phys.*, **143**, 1998, 90–124.
- [5] Moser, R. D., Kim, J. and Mansour, N. N., Direct numerical simulation of turbulent channel flow up to $Re_\tau = 590$, *Phys. Fluids*, **11**, 1999, 943–945.
- [6] Shiri, A. and George, W. K., Turbulent natural convection in a differentially heated vertical channel, *Proceedings of 2008 ASME Summer Heat Transfer Conference*.
- [7] Spalart, P. R., Moser, R. D. and Rogers, M. M., Spectra methods for the Navier–Stokes equations with one infinite and two periodic directions, *J. Comput. Phys.*, **96**, 1991, 297–324.
- [8] Tsuji, T. and Nagano, Y., Characteristics of a turbulent natural convection boundary layer along a vertical flat plate, *Int. J. Heat Mass Transfer*, **31**, 1988, 1723–1734.
- [9] Versteegh, T. A. M. and Nieuwstadt, F. T. M., A direct numerical simulation of natural convection between two infinite vertical differentially heated walls scaling laws and wall functions, *Int. J. Heat Mass Transfer*, **42**, 1999, 3673–3693.
- [10] Yuan, X., Moser, A. and Suter, P., Wall functions for numerical simulation of turbulent natural convection along vertical plates, *Int. J. Heat Mass Transfer*, **36**, 1993, 4477–4485.